universe

MDPI

Communication

Hamiltonian Approach to QCD at Finite Temperature †

Hugo Reinhardt *, Davide Campagnari and Markus Quandt

Institut für Theoretische Physik, Universität Tübingen, Auf der Morgenstelle 14, 72076 Tübingen, Germany; d.campagnari@uni-tuebingen.de (D.C.); markus.quandt@uni-tuebingen.de (M.Q.)

* Correspondence: hugo.reinhardt@uni-tuebingen.de

† This paper is based on the talk given by H. Reinhardt at the 7th International Conference on New Frontiers in Physics (ICNFP 2018), Crete, Greece, 4–12 July 2018.

Received: 24 October 2018; Accepted: 15 January 2019; Published: 22 January 2019

Abstract: A novel approach to the Hamiltonian formulation of quantum field theory at finite temperature is presented. The temperature is introduced by compactification of a spatial dimension. The whole finite-temperature theory is encoded in the ground state on the spatial manifold $S^1(L) \times \mathbb{R}^2$ where L is the length of the compactified dimension which defines the inverse temperature. The approach is then applied to the Hamiltonian formulation of QCD in Coulomb gauge to study the chiral phase transition at finite temperatures.

Keywords: gauge theory; finite temperature; variational approach; Hamiltonian picture

1. Introduction

The understanding of the QCD phase diagram is subject of intensive studies both experimentally and theoretically [1,2]. On the lattice, we have access to the finite-temperature behaviour of hadronic matter. The lattice methods developed thus far fail, however, at large chemical potential due to the notorious sign problem [3]. Therefore, non-perturbative continuum methods are needed. In the last 10–15 years, much effort has been undertaken to develop such non-perturbative continuum approaches. From the conceptual point of view, we can distinguish three basic approaches:

1. Dyson–Schwinger equations (DSE) [4–9];
2. Functional renormalization group flow equations [10,11];
3. Variational methods both in covariant form [12,13] and in the Hamiltonian formulation [14,15].

There are also semi-phenomenological approaches using a massive gluon propagator [16] or the Gribov–Zwanziger action [17,18]. In these proceedings, we discuss a variational Hamiltonian approach to QCD at finite temperature [14,15].

At finite temperature, the central quantity is the partition function and in the Hamiltonian approach this quantity is calculated as the trace of the grand canonical density operator $\exp(-H/T)$:

$$Z(L) = \mathrm{Tr}\, \mathrm{e}^{-H/T}, \tag{1}$$

where the chemical potential is set to zero for simplicity. For a quantum field theory, the Hamiltonian H contains interactions, which makes the treatment of the density operator very cumbersome and one usually resorts to a quasi-particle approximation for the Hamiltonian H in the exponent so that Wick's theorem can be used. There is, however, a much more efficient way to study quantum field theory at finite temperatures in the Hamiltonian formulation without explicitly calculating the whole partition function and thus without the need to introduce additional approximations to the density operator. This new approach [19] is based on the compactification of a spatial dimension. The finite temperature theory is fully encoded in the vacuum state on the partially compactified manifold $S^1(L) \times \mathbb{R}^2$. In the

following, we use this novel approach to study QCD at finite temperature. We first explain this approach and then apply it to the Hamilton formulation of QCD in Coulomb gauge to study the chiral phase transition. For this purpose, we first present the basic ingredients to the variational Hamiltonian approach to QCD in Coulomb gauge and summarize some essential zero-temperature results. Within this approach, we then study the quark sector at finite temperature where the focus is put on the chiral phase transition.

2. Finite Temperature from Compactification of a Spatial Dimension

The current standard approach to finite-temperature quantum field theory is to express the partition function (Equation (1)) by the functional integral

$$Z(L) = \int\limits_{b.c.} D(A,\psi) \exp\left[- \int\limits_{-L/2}^{L/2} dx^0 \int d^3x L_E(A,\psi) \right] , \tag{2}$$

where the bosonic (fermionic) fields satisfy (anti-)periodic boundary conditions in the Euclidean time

$$\begin{aligned} A(x^0 = L/2) &= A(x^0 = -L/2) , \\ \psi(x^0 = L/2) &= -\psi(x^0 = -L/2) . \end{aligned} \tag{3}$$

These boundary conditions compactify the Euclidean time axis to a circle with circumference L so that the space-time manifold of the finite-temperature theory is $S^1(L) \times \mathbb{R}^3$.

In a relativistic invariant quantum field theory, the Euclidean Lagrange density $L_E(A,\psi)$ is O(4) invariant. One can exploit this invariance to rotate the time axis onto a spatial axis and consequently one of the spatial axes onto the time axis, e.g.,

$$\begin{aligned} &x^0 \to x^3 , \quad A^0 \to A^3 , \quad \gamma^0 \to \gamma^3 , \\ &x^1 \to x^0 , \quad A^1 \to A^0 , \quad \gamma^1 \to \gamma^0 . \end{aligned} \tag{4}$$

A O(4) rotation transforms all Lorentz vectors in the same way, thus, together with the space time coordinates x^μ, we have also to rotate the gauge field A^μ and the Dirac matrices γ^μ. As a consequence of such an O(4) rotation, the temporal boundary conditions in Equation (3) become spatial boundary conditions

$$\begin{aligned} A(x^3 = L/2) &= A(x^3 = -L/2) , \\ \psi(x^3 = L/2) &= -\psi(x^3 = -L/2) . \end{aligned} \tag{5}$$

These boundary conditions compactify the 3-axis to a circle $S^1(L)$ so that the spatial manifold is now $S^1(L) \times \mathbb{R}^2$.

Reversing now the steps that lead from the partition function in the Hamiltonian form (Equation (1)) to the functional integral form (Equation (2)), which implies the canonical quantization on the spatial manifold $S^1(L) \times \mathbb{R}^2$, we obtain the representation [19]

$$Z(L) = \lim_{l\to\infty} \mathrm{Tr}\, \mathrm{e}^{-lH(L)} = \lim_{l\to\infty} \sum_n \mathrm{e}^{-lE_n(L)} , \tag{6}$$

where l denotes the length of the uncompactified spatial dimensions, which, of course, is infinity. Furthermore, $H(L)$ is the Hamiltonian on the spatial manifold $S^1(L) \times \mathbb{R}^2$ and $E_n(L)$ are its eigenvalues.

Note that, in the partition function (Equation (6)), the inverse temperature L no longer multiplies the Hamiltonian. Instead, the latter is defined on the spatial manifold $S^1(L) \times \mathbb{R}^2$ and thus temperature dependent. Since $l \to \infty$ from the sum over the energy eigenstates only the ground state survives

$$Z(L) = \lim_{l\to\infty} \exp(-lE_0(L))\,. \tag{7}$$

This argument requires that there is a mass gap between the ground state and the first excited state for the theory on $S^1(L)\times\mathbb{R}^2$, which we assume.[1] We have thus succeeded in expressing the entire partition function at inverse temperature L by the ground state energy $E_0(L)$ on the spatial manifold $S^1(L)\times\mathbb{R}^2$. The only assumptions made in the derivation of Equation (7) were

1. $O(4)$ invariance of the Euclidean Lagrange density, which should hold for any relativistically invariant theory. It does, however, not hold for a non-relativistic many-body system.
2. The absence of massless modes, i.e., the existence of a mass gap on the manifold $S^1(L)\times\mathbb{R}^2$. This is the generic case. For instance, QCD in the confining phase is known to develop such a gap, and this follows also self-consistently from the results in the next section. Extra caution may be required at temperatures above the deconfinement phase transition, where we can check our findings against thermal perturbation theory.

From the partition function (Equation (7)), we can derive the desired thermodynamic quantities in the standard fashion by taking derivatives. For the pressure P and energy density ε, we obtain

$$P = -\partial[Ve(L)]/\partial V\,, \qquad V = l^3\,, \tag{8}$$

$$\varepsilon = \partial[Le(L)]/\partial L - \mu\partial e(L)/\partial\mu\,, \tag{9}$$

where $e(L)$ is defined by separating the "spatial" volume Ll^2 from the ground state energy $E_0(L) = Ll^2e(L)$ and is referred to as pseudo-energy density. Finally, in the presence of a finite chemical potential for the fermions, the Dirac Hamiltonian receives an extra term [19]

$$h = \boldsymbol{\alpha}\boldsymbol{p} + \beta m \to h(L) = h + i\mu\alpha^3\,, \tag{10}$$

where α^3 is the Dirac matrix corresponding to the compactified space dimension.

As shown above, the whole finite-temperature quantum field theory can be entirely extracted from the vacuum state on the spatial manifold $S^1(L)\times\mathbb{R}^2$ and there is no need to explicitly calculate the partition function. In particular, no excited states have to be determined. However, one pays a price: on the spatial manifold $S^1(L)\times\mathbb{R}^2$, the usual O(3) invariance is, of course, broken to O(2), which will complicate the explicit calculations, e.g., the integral over a function in momentum space in $\mathbb{R}^3$, $\int d^3p f(\boldsymbol{p})$, is replaced on $S^1(L)\times\mathbb{R}^2$ by

$$\int_L d^3p f(\boldsymbol{p}) := \int d^2p_\perp \frac{2\pi}{L} \sum_{n=-\infty}^{\infty} f(\boldsymbol{p}_\perp, \omega_n)\,, \tag{11}$$

where

$$\omega_n = \begin{cases} \frac{2\pi n}{L} & , \quad \text{bosons} : n_F = 0 \\ \frac{(2n+1)\pi}{L} & , \quad \text{fermions} : n_F = 1 \end{cases} \tag{12}$$

are the Matsubara frequencies. For O(3)-invariant observables $f(\boldsymbol{p}) = f(|\boldsymbol{p}|)$, the three-dimensional integral $\int d^3p\, f(\boldsymbol{p})$ reduces to a one-dimensional integral over the modulus of the momentum with integrals over the angles being trivial, while on the spatial manifold $S^1(L)\times\mathbb{R}^2$ we have in addition a summation over the Matsubara frequencies and instead of the single function $f(|\boldsymbol{p}|)$ we have an (in principle infinite) set of functions $f(|\boldsymbol{p}_\perp|, \omega_n)$. Fortunately, as the temperature increases, fewer and fewer Matsubara frequencies have to be included and, in the high-temperature limit, only the lowest

[1] We thank the anonymous referee for pointing out this implicit assumption.

Matsubara frequency $\omega_{n=0}$ survives. For small temperatures, many Matsubara frequencies have to be included. In that case, however, it is more convenient to perform a Poisson resummation

$$\frac{1}{2\pi}\sum_{k=-\infty}^{\infty} \mathrm{e}^{ikx} = \sum_{n=-\infty}^{\infty} \delta(x-2\pi n) \tag{13}$$

by means of which the integral Equation (11) is converted to

$$\int\limits_{L} d^3p f(\boldsymbol{p}) = \int d^2p_\perp \int dp_3 f(\boldsymbol{p}_\perp, p_3) \sum_{k=-\infty}^{\infty} (-)^{n_F k} \exp(ikLp_3)\,. \tag{14}$$

The momentum integral is here the same as on $\mathbb{R}^3$ (i.e., as in the zero-temperature case). However, we have here in addition a summation over an index k of the oscillating function $\exp(ikLp_3)$, and the temperature enters explicitly only through this oscillating factor. The term with $k = 0$ is independent of the temperature and also agrees with the corresponding zero-temperature expression, i.e., the limit $L \to \infty$ in Equation (11). Here, an advantage of the Poisson resummed form Equation (14) becomes apparent: the zero-temperature vacuum contribution to an observable, which is usually divergent, can be easily extracted. In fact, in the zero-temperature limit $L \to \infty$, only the $k = 0$ term survives while the terms with $k \neq 0$ become rapidly oscillating functions that give zero contribution to any momentum integral. As the temperature increases more and more, terms $k \neq 0$ have to be included. For the study of a phase transition at finite temperature, it is convenient to do the calculations from both ends starting at zero temperature with the Poisson resummed form (Equation (14)) and at high temperature with the Matsubara sum (Equation (11)), and extend the calculations to an overlap regime containing the critical temperature where both approaches are applicable with a moderate number of terms included.

Let us illustrate this novel approach to Hamiltonian quantum field theory at finite temperatures by considering a gas of non-interacting massive bosons and fermions with a single particle energy

$$\omega(\boldsymbol{p}) = \sqrt{m^2 + \boldsymbol{p}^2}\,, \tag{15}$$

In the usual formulation of finite-temperature quantum field theory, the pressure of the Bose gas is given by

$$P = \frac{2}{3}\int \mathrm{đ}^3p\, \frac{\boldsymbol{p}^2}{\omega(\boldsymbol{p})}\, n(\boldsymbol{p}), \qquad n(\boldsymbol{p}) = \left(\mathrm{e}^{L\omega(\boldsymbol{p})} - 1\right)^{-1}, \tag{16}$$

where $n(\boldsymbol{p})$ are the finite-temperature Bose occupation numbers, and we use (here and in the following) the short-hand notation $\mathrm{đ}^n p = d^n p/(2\pi)^n$. In the novel approach presented above, one finds for the pressure from Equation (8) $P = -e(L)$, and the pseudo-energy density $e(L)$ for a free gas of bosons is given by their ground state energy density on $S^1(L) \times \mathbb{R}^2$

$$e(L) = \frac{1}{2}\int\limits_{L} \mathrm{đ}^3p\, \omega(\boldsymbol{p}) = \frac{1}{2}\int \mathrm{đ}^2p_\perp \frac{1}{L}\sum_{n=-\infty}^{\infty} \sqrt{\boldsymbol{p}_\perp^2 + \omega_n^2}\,. \tag{17}$$

The two expressions given by Equations (16) and (17) are certainly not identical. In fact, the last expression (Equation (17)) is even ill-defined. To make it well-defined, we first represent the square root in Equation (17) by a proper time integral, i.e., we set, for any $A > 0$,

$$\sqrt{A} = \frac{1}{\Gamma(-1/2)} \lim_{\Lambda\to\infty} \int\limits_{1/\Lambda^2}^{\infty} d\tau \tau^{-3/2} \mathrm{e}^{-\tau A}\,. \tag{18}$$

Then, the momentum integration can be carried out. Using the Poisson resummed form (Equation (14)), we obtain

$$e(L) = -\frac{1}{2\pi^2} \sum_{n=-\infty}^{\infty} \left(\frac{m}{nL}\right)^2 K_{-2}(nLm)\,, \tag{19}$$

where $K_{-2}(x) = K_2(x)$ is the modified Bessel function. The term with $n = 0$ represents the energy density of the Bose gas on $\mathbb{R}^3$. This is the usual vacuum $(T = 0)$ contribution, which is divergent and has to be omitted as usual. Taking in the remaining sum the limit $m \to 0$, we find for the pressure of the massless Bose gas

$$P = \frac{\xi(4)}{\pi^2} T^4 = \frac{\pi^2}{90} T^4\,, \tag{20}$$

which is the correct expression.

For a non-interacting Fermi gas, the pseudo-energy density is given by the energy of the Dirac sea on $S^1(L) \times \mathbb{R}^2$. For fermions with the energy $\omega(\boldsymbol{p})$ (Equation (15)) (on $\mathbb{R}^3$) at a finite chemical potential μ, we find by using Equation (10)

$$e(L) = -2 \int_L \mathrm{d}^3 p\, \omega(\boldsymbol{p}_\perp, p_3 + i\mu)\,, \tag{21}$$

where the factor of 2 comes from the two spin degrees of freedom. Repeating the manipulations as carried out in the Bosonic case, one finds

$$e(L) = -\frac{2}{\pi^2} \sum_{n=-\infty}^{\infty} \cos\left[nL\left(\frac{\pi}{L} - i\mu\right)\right] \left(\frac{m}{nL}\right)^2 K_{-2}(nLm)\,. \tag{22}$$

Again, we have to omit the $n = 0$ term, which represents the vacuum $T = 0$ contribution to the energy density. Even after removing the $n = 0$ term, the remaining sum is ill-defined. To make it well-defined, we continue the chemical potential to pure imaginary values, $i\mu \to x$, and use

$$\sum_{n=1}^{\infty} (-)^n \frac{\cos(nx)}{n^4} = \frac{1}{48}\left[-\frac{7}{15}\pi^4 + 2\pi^2 x^2 - x^4\right]\,. \tag{23}$$

Continuing the obtained result back to real chemical potentials, one finds for massless fermions

$$P = \frac{1}{12\pi^2}\left[\frac{7}{15}\pi^4 T^4 + 2\pi^2 T^2 \mu^2 + \mu^4\right]\,, \tag{24}$$

which is the correct expression.

In the following, we apply the approach to finite-temperature Hamiltonian quantum field theory [19] summarized above to QCD in Coulomb gauge, where we focus on the chiral phase transition at finite temperatures.

3. Hamiltonian Approach to QCD in Coulomb Gauge

3.1. Yang–Mills Sector

The Hamiltonian approach usually starts from the Weyl gauge $A_0 = 0$, which fixes the gauge up to time-independent gauge transformations. The latter can be conveniently fixed by using the Coulomb gauge $\boldsymbol{\partial A} = 0$, which has the advantage that Gauss' law can be explicitly resolved resulting in the gauge fixed Hamiltonian [20]

$$H = \frac{1}{2}\int \left(J^{-1}\boldsymbol{\Pi} J \boldsymbol{\Pi} + \boldsymbol{B}^2\right) + H_{\mathrm{C}}\,. \tag{25}$$

Here, $\Pi = \delta / i\delta \boldsymbol{A}$ is the momentum operator, which represents the color electric field, and $\boldsymbol{B}$ is the color magnetic field. The magnetic term $\boldsymbol{B}^2$ serves as a potential for the gauge field. Furthermore, $J = \mathrm{Det}(-\hat{D} \cdot \boldsymbol{\partial})$ is the Faddeev–Popov determinant, with $\hat{\boldsymbol{D}} = \boldsymbol{\partial} + g\hat{\boldsymbol{A}}$, $\hat{A}^{ab} = f^{acb}A^c$ being the covariant derivative in the adjoint representation of the gauge group denoted by the "hat". Finally,

$$H_{\mathrm{C}} = \frac{1}{2} \int J^{-1} \rho J (-\hat{\boldsymbol{D}} \cdot \boldsymbol{\partial})^{-1} (-\partial^2) (-\hat{\boldsymbol{D}} \boldsymbol{\partial})^{-1} \rho \tag{26}$$

is the so-called Coulomb term, which arises from the longitudinal part of the kinetic energy of the gauge field. Here,

$$\rho^a = -\hat{\boldsymbol{A}}^{ab} \boldsymbol{\Pi}^b + \rho_q^a, \qquad \rho_q^a = q^\dagger t^a q \tag{27}$$

is the color charge density, which contains, besides the color charge density of the quark fields, a gluonic term. Let us stress that in the gauge fixed Hamiltonian, Equation (25), Gauss' law has been exactly resolved, so gauge invariance is fully taken into account (at least as long as the Hamiltonian is treated exactly). In the gauge fixed theory, the Faddeev–Popov determinant J also enters the integration measure in the scalar product of wave functionals

$$\langle \phi | \ldots | \psi \rangle = \int DA \, J \, \phi^*[A] \ldots \psi[A], \tag{28}$$

where the integration runs over the transversal gauge fields only and must, in principle, be restricted to the so-called fundamental modular region.

The aim of the Hamiltonian approach is to solve the functional Schrödinger equation $H\psi[A] = E\psi[A]$ for the vacuum wave functional $\psi[A]$. In the Yang–Mills sector, we use the ansatz [14,15]

$$\psi[A] = \frac{1}{\sqrt{J}} \exp\left[-\frac{1}{2} \int A \omega A \right], \tag{29}$$

where $\omega(\boldsymbol{x}, \boldsymbol{y})$ is a variational kernel that is determined by minimizing the expectation value of the gauge fixed Hamiltonian (Equation (25)). Its Fourier transform represents the gluon energy since

$$\langle \psi | A_i(\boldsymbol{x}) A_j(\boldsymbol{y}) | \psi \rangle = \frac{1}{2} t_{ij}(x) \omega^{-1}(\boldsymbol{x}, \boldsymbol{y}) \tag{30}$$

with $t_{ij}(x) = \delta_{ij} - \partial_i \partial_j / \partial^2$ being the transverse projector.

The resulting gluon gap equation can be solved analytically in the infrared and, furthermore, was solved numerically in the entire momentum regime. The result is shown in Figure 1. The gluon energy $\omega(p)$ is infrared diverging signaling confinement, while it behaves at large momenta similar to the photon energy in agreement with asymptotic freedom. Figure 2 shows the lattice data for the static gluon propagator (Equation (30)) obtained in Ref. [21] together with the result of the variational calculation, both for the color group SU(2). One finds excellent agreement in the infrared and in the ultraviolet. However, in the mid-momentum regime, some strength is missing. The agreement with the lattice is considerably improved when a non-Gaussian ansatz for the vacuum wave functional is used, which contains in the exponent, besides the quadratic term, a cubic and quartic term (see [22]). Note also that the lattice results can be perfectly fitted by the so-called Gribov formula [17,21]

$$\omega(\boldsymbol{p}) = \sqrt{\boldsymbol{p}^2 + M^4 / \boldsymbol{p}^2} \tag{31}$$

with a Gribov mass $M \simeq 880\,\mathrm{MeV}$.

A central role in Gribov's confinement scenario [17] plays the ghost form factor $d(\boldsymbol{p})$, which is defined by

$$\langle \psi | (-\hat{\boldsymbol{D}} \boldsymbol{\partial})^{-1} | \psi \rangle = d / (-\Delta) \tag{32}$$

and embodies the non-Abelian features of Yang–Mills theory in the sense that it describes the deviation of the latter from electrodynamics where the ghost form factor is unity. It can be shown [23] that the inverse of this quantity represents the dielectric function of the Yang–Mills vacuum $\varepsilon(\boldsymbol{p}) = d^{-1}(\boldsymbol{p})$. By the so-called horizon condition $d^{-1}(0) = 0$, which is fulfilled by the lattice data and enters as a boundary condition in the variational calculation, the dielectric constant vanishes in the infrared making the Yang–Mills vacuum a perfect color dielectricum, which is nothing but a dual superconductor. In this way, Gribov's confinement scenario is directly connected with the dual Meissner effect of the magnetic monopole picture of confinement [24,25]. One can also show that the infrared divergence of the ghost form factor, i.e., the horizon condition, $d^{-1}(0) = 0$, disappears when one removes the so-called center vortices from the field configurations of the lattice functional integral, establishing also the connection of Gribov's scenario with the center vortex picture of confinement.

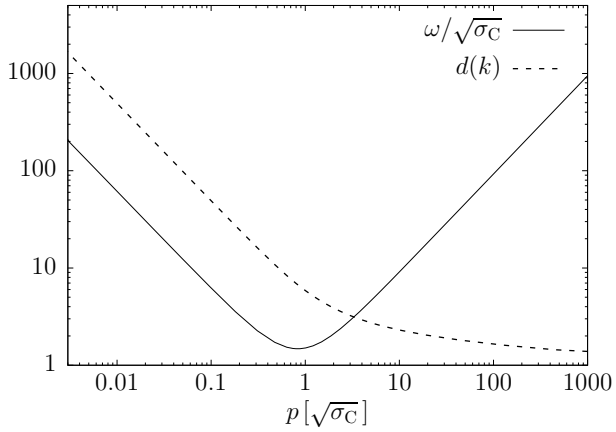

Figure 1. Numerical solution of the gluon energy (Equation (30)) $\omega(k)$ and the ghost form factor (32) $d(k)$.

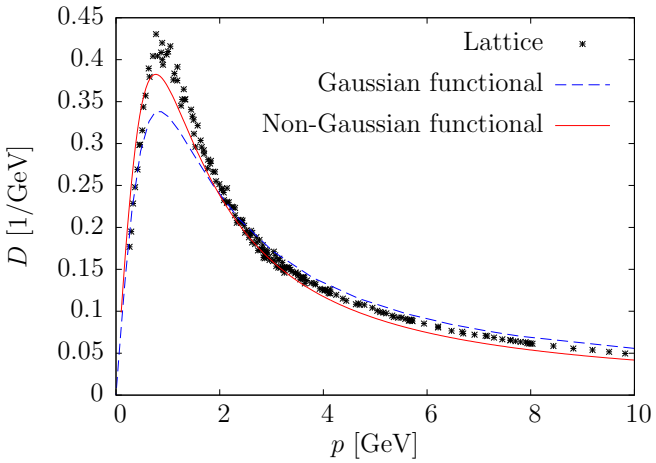

Figure 2. The static gluon propagator in Coulomb gauge calculated on the lattice for SU(2) gauge theory (crosses). The dashed and the full curves show the result of the variational calculation using, respectively, a Gaussian ansatz and a non-Gaussian ansatz for the vacuum wave functional.

In the quark contribution to the Coulomb term, the Faddeev–Popov determinant drops out and the Yang–Mills vacuum expectation value of the Coulomb term gives rise to a potential acting between the static color charges

$$V(\boldsymbol{x}, \boldsymbol{y}) = \langle \psi | (-\hat{\boldsymbol{D}} \cdot \boldsymbol{\partial})^{-1} (-\partial^2) (-\hat{\boldsymbol{D}} \cdot \boldsymbol{\partial})^{-1} | \psi \rangle \,. \tag{33}$$

This potential is shown in Figure 3. It behaves as an ordinary Coulomb potential at small distances but increases at large distances linearly with a coefficient σ_C, referred to as Coulomb string tension. It can be shown that the Coulomb string tension represents an upper bound to the Wilsonian string

tension [26] and, furthermore, that it is related not to the temporal but to the spatial string tension [27]. Similar to the latter, it increases with the temperature above the deconfinement phase transition.

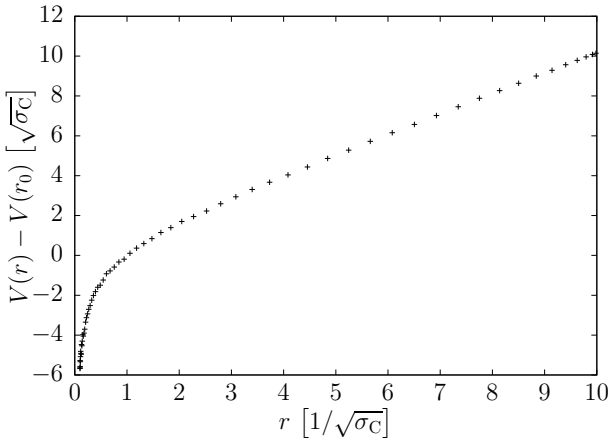

Figure 3. Non-Abelian Coulomb potential (Equation (33)) obtained in the variational approach [28].

3.2. Quark Sector

When the quarks are included, one has to keep the quark part ρ_q in the color charge density (Equation (27)) and add the Dirac Hamiltonian

$$H_q = \int d^3x\, q^\dagger(x)\,[\boldsymbol{\alpha}(\boldsymbol{p} + g\boldsymbol{A}(x)) + \beta m_0]\, q(x)\,, \tag{34}$$

where $\boldsymbol{\alpha}, \beta$ are the usual Dirac matrices and m_0 denotes the current mass of the quarks, which we will ignore in the following.[2] For the vacuum wave functional of the quarks, the following ansatz

$$\langle A|\phi\rangle = \exp\left\{\int q_+^\dagger \left[s\beta + (v + w\beta)\boldsymbol{\alpha}\cdot\boldsymbol{A}\right] q_-\right\} \tag{35}$$

is used, where $q_\pm$ denotes the positive and negative energy part of the quark field and s, v, and w are variational kernels. This ansatz contains explicitly the coupling of the quarks to the spatial gluons. When this coupling is neglected, $v = w = 0$, the ansatz (Equation (35)) reduces to the BCS type wave functional considered in Refs. [29–31]. As shown below, the inclusion of the coupling of the quarks to the spatial gluons is absolutely necessary to reproduce the phenomenological value of the quark condensate, as shown in Ref. [32] where the ansatz (Equation (35)) with $w = 0$ was used. The advantage of keeping both Dirac structures in the quark gluon coupling in Equation (35) is that all UV divergences cancel in the resulting variational equations, see refs. [33,34]. The variational equations for v and w can be explicitly solved in terms of the scalar kernel s and the gluon energy ω. For the quark sector, one finds then a single non-linear equation, which is conveniently expressed in terms of the effective quark mass

$$M(\boldsymbol{p}) = \frac{2|\boldsymbol{p}|\, s(\boldsymbol{p})}{1 - s^2(\boldsymbol{p})}. \tag{36}$$

In the numerical calculation, we use for the static quark potential (Equation (33))

$$V_C(|\boldsymbol{p}|) = \frac{g^2}{\boldsymbol{p}^2} + \frac{8\pi\sigma_C}{(\boldsymbol{p}^2)^2} \tag{37}$$

---

[2] Although we only consider a single massless quark flavor in this section, the results easily generalize to the case of N_f massless flavors. In fact, the only change in this case would be an additional factor N_f in the chiral condensate, which drops out when forming the ratios in Figures 7 and 8. The results of this section are therefore independent of N_f (as long as the quark flavors are massless), and it is sufficient to study $N_f = 1$.

with the Coulomb string tension σ_C defining the scale of the theory. Furthermore, the quark-gluon coupling constant g, which is the same as in Equation (34), is chosen to reproduce the phenomenological value of the quark condensate

$$\langle \bar{q}q \rangle = (-235\,\mathrm{MeV})^3\,, \tag{38}$$

which requires $g \simeq 2.1$ for the value $\sigma_C = 2.5\sigma$ of the Coulomb string tension favored by our lattice calculation [21]. This corresponds to $\alpha = g^2/4\pi \approx 0.35$ at the chiral symmetry breaking scale. The resulting effective quark mass is shown in Figure 4 as function of the momentum. For sake of comparison we also show the mass function that is obtained when the coupling of the quarks to the spatial gluons as well as the perturbative part of the Coulomb potential (Equation (37)) is omitted $(g = 0)$. Both curves agree in the infrared which is due to the fact that this regime is exclusively determined by the Coulomb potential (Equation (37)). The two curves differ substantially only in the ultraviolet. This part gives, however, a significant contribution to the quark condensate. If the coupling of the quarks to the spatial gluons is omitted $(g = 0)$, one finds a quark condensate of

$$\langle \bar{q}q \rangle = (-185\,\mathrm{MeV})^2 \tag{39}$$

when the Coulomb string tension is chosen as before $(\sigma_C = 2.5\sigma)$. The infrared value of the effective quark mass $M(0) = 140$ MeV seems to be substantially too small compared to the effective mass extracted from the quark propagator calculated in Landau gauge on the lattice and in Dyson–Schwinger calculations. However, it is shown in Ref. [35] that the effective quark mass extracted from the static quark propagator is significantly smaller than the one obtained from the four-dimensional propagator (see Figure 5).

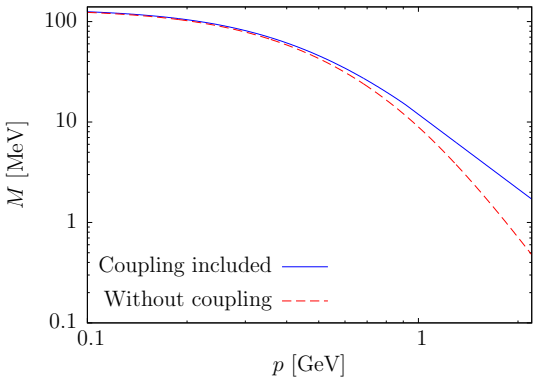

Figure 4. Mass function obtained from the (quenched) solution of the quark gap equation. Results are presented for $g \simeq 2.1$ (full curve) and $g = 0$ (dashed curve).

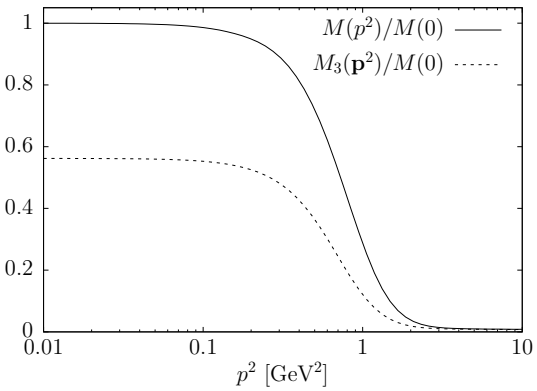

Figure 5. Comparison between the full mass function $M(p^2)$ in Landau gauge (continuous line) and the mass function $M_3(\mathbf{p}^2)$ of the equal-time propagator (dashed line) (see [35]).

The results obtained thus far at zero temperature within the Hamiltonian approach to QCD in Coulomb gauge are rather encouraging to warrant also the extension to finite temperatures in the novel approach presented in Section 2.

4. QCD at Finite Temperatures

The extension of the above-presented Hamiltonian approach to QCD in Coulomb gauge to finite temperatures is straightforward, but numerically much more expensive: a single integral equation from the approach at zero temperature becomes a coupled set of integral equations at finite temperature, where each included Matsubara frequency gives rise to a separate equation. To reduce the numerical expense, in the following, we consider only the quark sector where we neglect the coupling of the quarks to the spatial gluons. In the approximation considered in Section 3.2, the quark sector then decouples from the Yang–Mills sector. The influence of the Yang–Mills sector is then completely contained in the non-abelian Coulomb potential (Equation (33)), which, for simplicity, we replace by its infrared limit given in Equation (37) with $g = 0$. The quark Hamiltonian then reduces to

$$H = \int \mathrm{d}^3x\, q^\dagger(\boldsymbol{x})\boldsymbol{\alpha}\cdot\boldsymbol{p}q(\boldsymbol{x}) + \frac{1}{2}\int \mathrm{d}^3x \int \mathrm{d}^3y\, \rho(\boldsymbol{x})\, V_{\mathrm{C}}(\boldsymbol{x}-\boldsymbol{y})\, \rho(\boldsymbol{y}), \qquad \rho^a(\boldsymbol{x}) = q^\dagger(\boldsymbol{x})t^a q(\boldsymbol{x}), \tag{40}$$

which, in fact, is the model considered in Refs. [29,30]. The corresponding functional Schrödinger equation is then solved variationally with the ansatz (Equation (35)) with $v = w = 0$, resulting in the quark gap equation

$$M(\boldsymbol{p}) = \frac{C_F}{2}\int\limits_L \frac{d^3q}{(2\pi)^3} V_{\mathrm{C}}(|\boldsymbol{p}-\boldsymbol{q}|)\frac{M(\boldsymbol{q}) - M(\boldsymbol{p})\hat{\boldsymbol{p}}\cdot\hat{\boldsymbol{q}}}{\sqrt{\boldsymbol{q}^2 + M(\boldsymbol{q})}} \tag{41}$$

for the effective quark mass(Equation (36)) where the finite-temperature integration measure is defined in Equation (11) and we have used the shorthand notation $M(\boldsymbol{p}) \equiv M(\boldsymbol{p}_\perp, \omega_n)$. The prefactor $C_F = (N_c^2 - 1)/(2N_c)$ is the quadratic Casimir of the colour group $SU(N_c)$.

We have solved the gap Equation (41) in the Matsubara form (Equation (11)) starting at high temperatures and in the Poisson resummed form (Equation (14)) given by

$$M(\boldsymbol{p}) = \frac{C_F}{2}\sum_{k=-\infty}^{\infty}(-1)^k \int \frac{d^3q}{(2\pi)^3}\, V_{\mathrm{C}}(\boldsymbol{q})\cos\big(\beta k(q_z + p_z)\big)\, \frac{M(\boldsymbol{q}) - \big[1 + \frac{\boldsymbol{p}\cdot\boldsymbol{q}}{\boldsymbol{p}^2}\big]M(\boldsymbol{p})}{\sqrt{(\boldsymbol{q}+\boldsymbol{p})^2 + M(\boldsymbol{q}+\boldsymbol{p})}}\,. \tag{42}$$

This form is most convenient for small temperatures where only a few terms of the Poisson sum have to be included (remember the $k = 0$ term represents the zero-temperature contribution, as explained in Section 2). The numerical expense is larger for the Poisson resummed form due to the oscillating behaviour of the integrand. However, it is advantageous in the sense that it is manifestly infrared finite. In the Matsubara form (Equation (41)), a spurious infrared singularity appears when the sum over Matsubara frequencies is restricted to a finite number of terms. When the Matsubara sum is carried out to infinite order (which effectively is done in the Poisson resummed form), the infrared singularity disappears. Therefore, the numerical solution of the gap equation in the Matsubara frequency representation has to be done with great care. We solve the Poisson resummed form starting from zero temperature until above the chiral phase transition regime and solve Equation (41) in the Matsubara representation at large to moderate temperatures below the deconfinement phase transition [36]. There is a broad overlap regime where both representations can be used and yield the same result. Figure 6 shows the resulting effective quark mass at finite temperatures for two extreme cases of the orientation of the external momentum relative to the compactified dimension. Compared to the zero-temperature solution, there is a substantial reduction in the infrared mass already well below the temperatures where the phase transition occurs. This reduction of the effective quark mass has, however, little effect on the quark condensate until near the phase transition regime. This can be seen in Figure 7 where the quark condensate is shown as function of the temperature. The figure

contains both the results from the Matsubara representation as well as from the Poisson resummed form of the gap equation. Both results agree very well in a broad transition regime where the chiral phase transition occurs. This transition is seen to be of second order. From the numerical data, one extracts a critical temperature of

$$T_\chi = 0.13\sqrt{\sigma_C}\,. \tag{43}$$

Using for the Coulomb string tension the value favored by our lattice calculations $\sigma_C = 2.5\sigma$, one finds a critical temperature of $T_\chi \simeq 92\,\mathrm{MeV}$. This temperature is too small compared to the lattice result $T_\chi^{lat} = 155\,\mathrm{MeV}$. A smaller critical temperature is expected from the present calculations since we have neglected the coupling of the quarks to the spatial gluons. As shown in Section 3.2, this coupling increases the value of the chiral quark condensate. If we choose the Coulomb string tension to reproduce the phenomenological value of the quark condensate (Equation (38)), which requires $\sigma_C = 4.1\sigma$, we find indeed a substantial larger critical temperature of $T_\chi = 115\,\mathrm{MeV}$ which, however, is still too small compared to the lattice result. One should notice, however, that, in the Adler–Davis model considered here, the temperature effects of the gluon sector are completely ignored. In particular, the Coulomb string tension is known to increase with the temperature [27] resulting via Equation (43) in an increase in the critical temperature of the chiral phase transition. Furthermore, in the present calculations, we have neglected the ultraviolet part of the non-Abelian Coulomb potential whose effect on the critical temperature is, however, difficult to estimate.

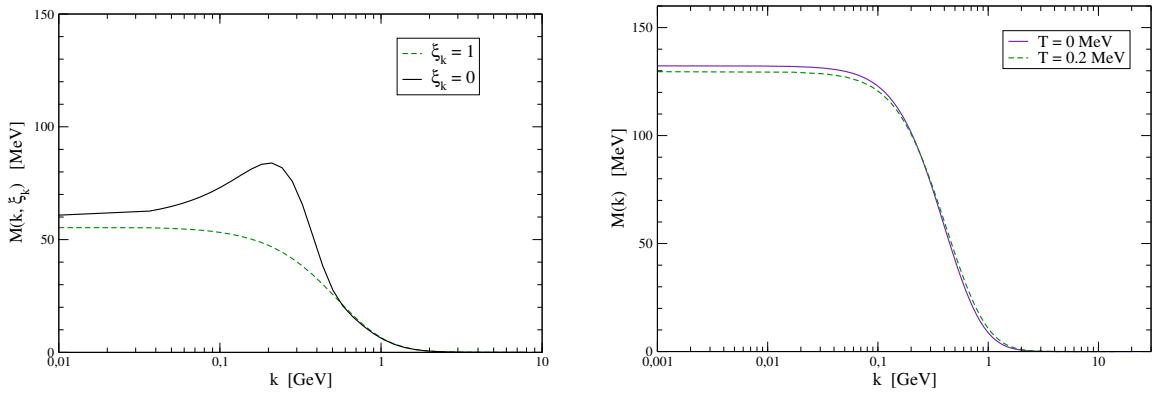

Figure 6. (**Left**) Mass function $M(k, \xi_k)$ at $T = 80\,\mathrm{MeV}$ with the momentum $\boldsymbol{k}$ pointing in various directions relative to the heat bath. (**Right**) Mass function $M(k, 1)$ for small temperatures compared to the $T = 0$ limit.

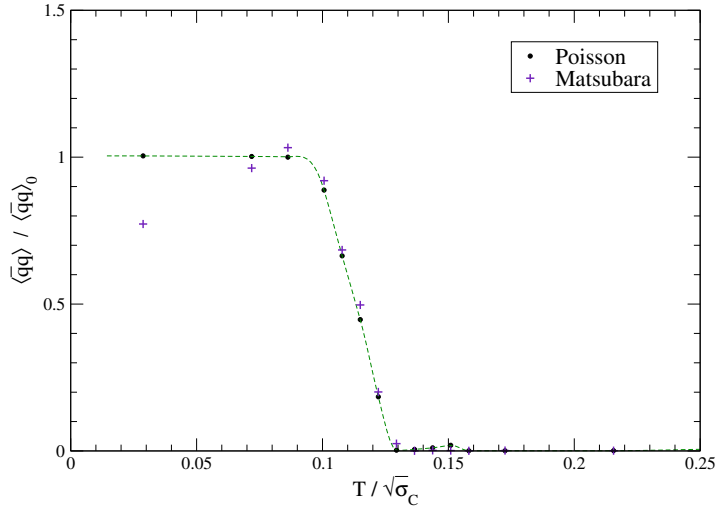

Figure 7. Chiral condensate as a function of the temperature, from both the Matsubara and Poisson formulations. To guide the eye, a dashed line was added through the Poisson data from which the critical temperature is determined.

Let us also mention that in the canonical finite-temperature Hamiltonian approach where a quasi-particle ansatz is assumed for the Hamiltonian in the grand canonical density operator $\exp(-H/T)$, one finds an even smaller critical temperature of $T_\chi = 0.091\sqrt{\sigma_C}$. Finally, Figure 8 shows the quark condensate as function of the temperature when one uses the zero-temperature solution of the quark gap equation. As one can see, this approximation is valid below the phase transition regime but fails completely as the temperature approaches the transition regime. The chiral condensate calculated with the zero-temperature solution decreases only slowly with the temperature and does not show a second-order phase transition.

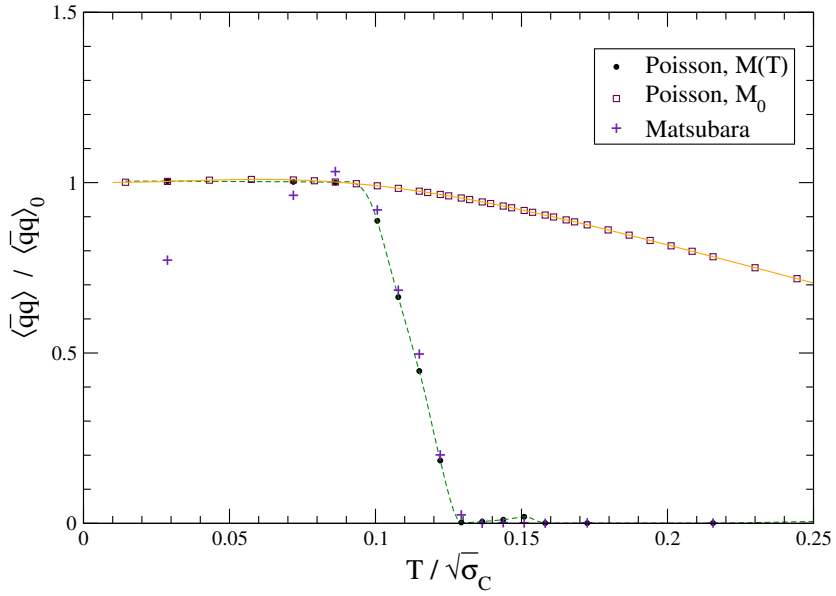

Figure 8. The quark condensate as function of the temperature calculated from the zero- and finite-temperature solutions of the quark gap equation.

The novel approach to finite temperatures within the Hamiltonian formulation assumes O(4) invariance of the Euclidean field theory. This implies that all components of the gauge field are treated on equal footing. This is certainly not the case for the Adler–Davis model. The potential term arises from the correlator of the temporal gluons while the spatial gluons are neglected in this model. The present approach to finite-temperature Hamiltonian quantum field theory, which assumes O(4) invariance including covariance in the treatment of the gauge fields, when applied to the Adler-Davis model in fact yields the thermodynamics of the covariant extension of this model. Thus, the present approach is not only superior in the sense that it does not require additional approximation to the grand canonical density operator but also yields automatically the finite-temperature theory of the covariant extension of a non-covariant model field theory. In general, the present approach when applied to a non-relativistic invariant theory (i.e., non O(4) invariant theory in Euclidean space) yields the finite-temperature theory of a relativistic extension.

5. Conclusions

In these proceedings, we have presented a novel approach to the Hamiltonian formulation of quantum field theory at finite temperatures by compactifying a spatial dimension. We have shown that this method agrees with the results of the traditional canonical approach when exact (analytic) calculations are possible. The technique is advantageous over the traditional one since it does not require an explicit calculation of the trace of the grand canonical density operator, which in an interacting quantum field theory is difficult to handle and necessitates further approximations. Rather, in the novel approach, the complete finite-temperature theory is encoded in the vacuum state on the spatial manifold $S^1(L) \times \mathbb{R}^2$ with one dimension compactified to a circle $S^1(L)$. The circumference

of the circle represents the inverse temperature. In Ref. [37], this novel approach has been used to calculate the effective potential of the Polyakov loop in pure Yang–Mills theory using, however, the zero-temperature gluon and ghost propagator. The correct order of the deconfinement phase transition (second order for SU(2) and first order for SU(3)) were obtained with critical temperatures in the range between 270 MeV and 290 MeV. Unfortunately, these calculations were done using the zero-temperature variational solution of the Yang–Mills Schrödinger equation. These calculations should be repeated using the finite-temperature variational solutions. At the moment, we calculate the effective potential of the Polyakov loop including the quark Coulomb term, which is crucial in the quark sector as we have seen in the study of the chiral phase transition. When the infrared part of the non-Abelian Coulomb potential (Equation (37)) is neglected, one does not find spontaneous breaking of chiral symmetry for reasonable values of the coupling of the quarks to the spatial gluons. Therefore, this term is absolutely necessary for the description of the infrared behaviour of the quark sector and should hence also be included in the calculation of the effective potential of the Polyakov loop, the order parameter of confinement. Finally, the present approach should be extended to finite quark chemical potential, which is the regime of most interest in the QCD phase diagram.

Author Contributions: This work is a report on an ongoing research activity to which the authors contributed in equal parts. Original draft preparation: H.R., visualization: D.C. and M.Q., writing—review and editing: M.Q.

Funding: This work was supported in part by DFG under contract RE 856/9-2 and RE 856/10-1.

Conflicts of Interest: The authors declare no conflict of interest.

References

1. Karsch, F. Lattice QCD at high temperature and density. *Lect. Notes Phys.* **2002**, *583*, 209–249.
2. Fukushima, K.; Hatsuda, T. The phase diagram of dense QCD. *Rep. Prog. Phys.* **2011**, *74*, 014001. [CrossRef]
3. Gattringer, C.; Langfeld, K. Approaches to the sign problem in lattice field theory. *Int. J. Mod. Phys.* **2016**, *A31*, 1643007. [CrossRef]
4. Fischer, C.S. Infrared properties of QCD from Dyson-Schwinger equations. *J. Phys.* **2006**, *G32*, R253–R291. [CrossRef]
5. Alkofer, R.; von Smekal, L. The Infrared behavior of QCD Green's functions: Confinement dynamical symmetry breaking, and hadrons as relativistic bound states. *Phys. Rep.* **2001**, *353*, 281. [CrossRef]
6. Binosi, D.; Papavassiliou, J. Pinch Technique: Theory and Applications. *Phys. Rep.* **2009**, *479*, 1–152. [CrossRef]
7. Watson, P.; Reinhardt, H. Propagator Dyson-Schwinger Equations of Coulomb Gauge Yang-Mills Theory Within the First Order Formalism. *Phys. Rev. D* **2007**, *75*, 045021. [CrossRef]
8. Watson, P.; Reinhardt, H. Two-point functions of Coulomb gauge Yang-Mills theory. *Phys. Rev. D* **2008**, *77*, 025030. [CrossRef]
9. Watson, P.; Reinhardt, H. Slavnov-Taylor identities in Coulomb gauge Yang-Mills theory. *Eur. Phys. J.* **2010**, *C65*, 567–585. [CrossRef]
10. Pawlowski, J.M. Aspects of the functional renormalisation group. *Ann. Phys.* **2007**, *322*, 2831–2915. [CrossRef]
11. Gies, H. Introduction to the functional RG and applications to gauge theories. *Lect. Notes Phys.* **2012**, *852*, 287–348.
12. Quandt, M.; Reinhardt, H.; Heffner, J. Covariant variational approach to Yang-Mills theory. *Phys. Rev. D* **2014**, *89*, 065037. [CrossRef]
13. Quandt, M.; Reinhardt, H. A covariant variational approach to Yang-Mills Theory at finite temperatures. *Phys. Rev. D* **2015**, *92*, 025051. [CrossRef]
14. Feuchter, C.; Reinhardt, H. Variational solution of the Yang-Mills Schrödinger equation in Coulomb gauge. *Phys. Rev. D* **2004**, *70*, 105021. [CrossRef]
15. Reinhardt, H.; Feuchter, C. Yang-Mills wave functional in Coulomb gauge. *Phys. Rev. D* **2005**, *71*, 105002. [CrossRef]

16. Reinosa, U.; Serreau, J.; Tissier, M.; Wschebor, N. Deconfinement transition in SU(2) Yang-Mills theory: A two-loop study. *Phys. Rev. D* **2015**, *91*, 045035. [CrossRef]
17. Gribov, V. Quantization of non-Abelian gauge theories. *Nucl. Phys. B* **1978**, *139*, 1–19. [CrossRef]
18. Canfora, F.E.; Dudal, D.; Justo, I.F.; Pais, P.; Rosa, L.; Vercauteren, D. Effect of the Gribov horizon on the Polyakov loop and vice versa. *Eur. Phys. J.* **2015**, *C75*, 326. [CrossRef]
19. Reinhardt, H. Hamiltonian finite-temperature quantum field theory from its vacuum on partially compactified space. *Phys. Rev. D* **2016**, *94*, 045016. [CrossRef]
20. Christ, N.H.; Lee, T.D. Operator ordering and Feynman rules in gauge theories. *Phys. Rev. D* **1980**, *22*, 939–958. [CrossRef]
21. Burgio, G.; Quandt, M.; Reinhardt, H. Coulomb-Gauge Gluon Propagator and the Gribov Formula. *Phys. Rev. Lett.* **2009**, *102*, 032002. [CrossRef]
22. Campagnari, D.R.; Reinhardt, H. Non-Gaussian wave functionals in Coulomb gauge Yang-Mills theory. *Phys. Rev. D* **2010**, *82*, 105021. [CrossRef]
23. Reinhardt, H. Dielectric Function of the QCD Vacuum. *Phys. Rev. Lett.* **2008**, *101*, 061602. [CrossRef] [PubMed]
24. Hooft, G. Magnetic Monopoles in Unified Gauge Theories. *Nucl. Phys.* **1974**, *B79*, 276–284. [CrossRef]
25. Mandelstam, S. Vortices and Quark Confinement in Nonabelian Gauge Theories. *Phys. Rep.* **1976**, *23*, 245–249. [CrossRef]
26. Zwanziger, D. No Confinement without Coulomb Confinement. *Phys. Rev. Lett.* **2003**, *90*, 102001. [CrossRef] [PubMed]
27. Burgio, G.; Quandt, M.; Reinhardt, H.; Vogt, H. Coulomb versus physical string tension on the lattice. *Phys. Rev. D* **2015**, *92*, 034518. [CrossRef]
28. Epple, D.; Reinhardt, H.; Schleifenbaum, W. Confining solution of the Dyson-Schwinger equations in Coulomb gauge. *Phys. Rev. D* **2007**, *75*, 045011. [CrossRef]
29. Finger, J.R.; Mandula, J.E. Quark pair condensation and chiral symmetry breaking in QCD. *Nucl. Phys. B* **1982**, *199*, 168–188. [CrossRef]
30. Adler, S.; Davis, A. Chiral symmetry breaking in Coulomb gauge QCD. *Nucl. Phys. B* **1984**, *244*, 469–491. [CrossRef]
31. Alkofer, R.; Amundsen, P. Chiral symmetry breaking in an instantaneous approximation to Coulomb gauge QCD. *Nucl. Phys. B* **1988**, *306*, 305–342. [CrossRef]
32. Pak, M.; Reinhardt, H. Quark sector of the QCD groundstate in Coulomb gauge. *Phys. Rev. D* **2013**, *88*, 125021. [CrossRef]
33. Vastag, P.; Reinhardt, H.; Campagnari, D. Improved variational approach to QCD in Coulomb gauge. *Phys. Rev. D* **2016**, *93*, 065003. [CrossRef]
34. Campagnari, D.R.; Ebadati, E.; Reinhardt, H.; Vastag, P. Revised variational approach to QCD in Coulomb gauge. *Phys. Rev. D* **2016**, *94*, 074027. [CrossRef]
35. Campagnari, D.; Reinhardt, H. Variational and Dyson–Schwinger Equations of Hamiltonian Quantum Chromodynamics. *Phys. Rev. D* **2018**, *97*, 054027. [CrossRef]
36. Quandt, M.; Ebadati, E.; Reinhardt, H.; Vastag, P. Chiral symmetry restoration at finite temperature within the Hamiltonian approach to QCD in Coulomb gauge. *arXiv* **2018**, arXiv:1806.04493.
37. Reinhardt, H.; Heffner, J. Effective potential of the confinement order parameter in the Hamiltonian approach. *Phys. Rev. D* **2013**, *88*, 045024. [CrossRef]